INSTITUTE OF MATHEMATICS

THE CZECH ACADEMY OF SCIENCES

On the approximation of a virtual coarse space for domain decomposition methods in two dimensions

Juan Gabriel Calvo

Preprint No. 31-2017

PRAHA 2017

ON THE APPROXIMATION OF A VIRTUAL COARSE SPACE FOR DOMAIN DECOMPOSITION METHODS IN TWO DIMENSIONS

JUAN G. CALVO *

Abstract. A new extension operator for a virtual coarse space is presented which can be used in domain decomposition methods for nodal elliptic problems in two dimensions. In particular, a two-level overlapping Schwarz algorithm is considered and a bound for the condition number of the preconditioned system is obtained. This bound is independent of discontinuities across the interface. The extension operator saves computational time compared to previous studies where discrete harmonic extensions are required and it is suitable for general polygonal meshes and irregular subdomains. Numerical experiments that verify the result are shown, including some with regular and irregular polygonal elements and with subdomains obtained by a mesh partitioner.

Key words. domain decomposition, overlapping Schwarz algorithms, nodal elliptic problems, irregular subdomain boundaries, virtual element methods

AMS subject classifications. 65F08, 65F10, 65N30, 65N55

1. Introduction.

We will consider the scalar elliptic problem in two dimensions

$$-\nabla\cdot(\rho(\boldsymbol{x})\nabla u(\boldsymbol{x})) = f(\boldsymbol{x}), \quad \boldsymbol{x}\in\Omega, \quad \rho(\boldsymbol{x})>0, \quad f\in L^2(\Omega), \tag{1}$$

posed in $H^1(\Omega) := \{v\in L^2(\Omega) : \|\nabla v\|_{L^2(\Omega)} < \infty\}$ and with homogeneous Dirichlet boundary conditions. We will work as usual with a weak formulation for problem (1), namely: Find $u\in H^1_0(\Omega)$ such that

$$a(u,v) = F(v) \quad \forall\ v\in H^1_0(\Omega), \tag{2}$$

where $a(u,v) := \int_\Omega \rho\ \nabla u\cdot\nabla v\ d\boldsymbol{x}$, $F(v) := (f,v)_{0,\Omega}$ is the inner product in $L^2(\Omega)$ and $H^1_0(\Omega)$ is the subspace of $H^1(\Omega)$ with vanishing trace.

We consider a general polygonal triangulation $\mathcal{T}_h$ of Ω and discretize problem (2) with the novel Virtual Element Method (VEM) [1, 2]. The associated stiffness matrix is then obtained by defining a finite-dimensional space V_h and an computable, consistent and stable bilinear form $a_h(\cdot,\cdot)$ defined in $V_h\times V_h$.

We then construct a two-level overlapping additive Schwarz preconditioner for the associated linear system; see, e.g., [18, Chapter 3]. These methods were introduced in [10, 11, 12]. For this purpose, the domain Ω is decomposed in N non-overlapping subdomains $\{\Omega_i\}_{i=1}^N$ of diameter H_i which are the union of elements of the triangulation $\mathcal{T}_h$. The preconditioner has local contributions that correspond to homogeneous Dirichlet solvers on extensions $\Omega_i'\supset\Omega_i$, and a coarse component that involves a global solver of modest size. The dimension of our coarse space is equal to the number of subdomain vertices (the nodes of the triangulation that belong to three or more subdomains).

In general, there is no straightforward approach to define coarse basis functions in the presence of irregular subdomains. In this setting, the virtual space seems to be a natural choice since it can accommodate polygonal elements with no complications. Thus, general polygonal subdomains can be considered in the decomposition. Furthermore, the lowest-order space is characterized by functions that are harmonic in the interior of the subdomains, which have minimum H^1-seminorm amog the functions with the same values on the boundary. We note that previous studies related to

*Institute of Mathematics, Czech Academy of Sciences, Žitná 25, Praha 01, 110 01. (calvo@math.cas.cz). The author gratefully acknowledges the institutional support RVO 67985840.

irregular subdomains are based on discrete harmonic extensions starting with [8]; see also [7, 16, 19, 9] where John [13] and Jones [14] subdomains are considered.

Our virtual coarse space was introduced in [6], where two variants were considered: the full coarse virtual space V_0 defined on the partition $\{\Omega_i\}$ of Ω, and a reduced version $V_0^R \subset V_0$. In the VEM terminology, functions are virtual in the sense that they are never required to be constructed explicitly; the only available information is their degrees of freedom. Hence, in order to compute the coarse component of our preconditioner, we need to approximate the coarse functions in the virtual element space.

The first approach considered in [6] consists in defining the operator $R_0^T : V_0^R \to V_h$ by evaluating a piecewise linear interpolant. In the present study, we modify this operator and consider polynomial approximations inside the subdomains (with degree greater than or equal to two). These projectors are used in the VEM methods when assembling the stiffness matrices and can be computed by only knowing the degrees of freedom of the virtual functions. They provide a good approximation and allow to deduce a similar upper bound for the condition number of the preconditioned system. The bound obtained in Theorem 4.1 is also independent of discontinuities of ρ across the interface, and we will assume that ρ is constant in each subdomain Ω_i.

We note that the main advantage of our approach with respect to previous studies is that no discrete harmonic extensions are required in the algorithm, saving computational time. We also aim to contribute and enrich the literature related to iterative solvers for VEM discretizations, since there is a lack of theoretical analysis for such problems.

The rest of this paper is organized as follows. In Section 2 we introduce the notation that will be used throughout our analysis. In Section 3 we present the basic theory of VEM and the discretization of our problem. The coarse space is described in Section 4 along with the new extension operators that approximate the coarse basis functions. Then, Section 5 includes some technical tools and the proof of the bound for the condition number of the preconditioned system. We include some implementation details and report on some numerical experiments in Section 6. Finally, we present some closing remarks in Section 7.

2. Notation. Given $h > 0$, we will divide the domain Ω into simply connected polygons K (not necessarily similar) of diameter $h_K \leq h$; see some examples in Section 6. These polygons will be called elements and later we will introduce two assumptions on them. This polygonal triangulation will be called *fine mesh* and will be denoted by $\mathcal{T}_h$. The *set of nodes* of a partition $\mathcal{T}_h$ contains the vertices of all the elements $K \in \mathcal{T}_h$ and will be represented by $S_{\mathcal{N}}$, while the set $S_{\mathcal{N}}^K$ will include the nodes of $\mathcal{T}_h$ that are on the boundary of K. We note that the set $S_{\mathcal{N}}^K$ can contain, besides vertices of K, also hanging nodes, i.e., vertices of other polygons that lie on an edge of K. The bilinear form (2) restricted to an element K will be denoted by

$$a^K(u,v) := \int_K \rho \, \nabla u \cdot \nabla v \, d\boldsymbol{x}.$$

Furthermore, the domain Ω will be partitioned into N non-overlapping and simply connected subdomains $\{\Omega_i\}_{i=1}^N$ of diameter H_i which are the union of elements of the triangulation $\mathcal{T}_h$; see, e.g., Figure 1. The partition formed by $\{\Omega_i\}$ will be called *coarse mesh* and will be denoted by $\mathcal{T}_H$. In a similarly way, the set of nodes of $\mathcal{T}_H$ contains the vertices of all the subdomains Ω_i and will be represented by $S_{\mathcal{N}}^H$, while the set $S_{\mathcal{N}}^{\Omega_i}$ will include only the nodes of $\mathcal{T}_H$ that are on the boundary of Ω_i. Again,

hanging nodes are allowed on the coarse mesh. We will assume also that the coefficient $\rho(\boldsymbol{x})$ is constant and equal to ρ_i inside each subdomain Ω_i. We will then construct overlapping subdomains $\Omega_i' \supset \Omega_i$ by adding layers of elements that are external to Ω_i, and we will denote by δ_i the maximum width of the region $\Omega_i' \setminus \Omega_i$.

We will also partition the set of nodes $S_{\mathcal{N}}$ into disjoint sets. The nodes that belong to exactly one subdomain Ω_i are its *interior nodes*. A *subdomain edge* $\mathcal{E}^{ij}$ will be the interior of the intersection of the closure of two neighboring subdomains Ω_i and Ω_j. If such intersection has more than one component, each open component will be considered as a subdomain edge. Then, the endpoint nodes of $\mathcal{E}^{ij}$ will belong to the set of *subdomain vertices*, which will be denoted by $S_{\mathcal{V}}$. We will write $\mathcal{E}$ instead of $\mathcal{E}^{ij}$ if there is no need to identify the two subdomains Ω_i and Ω_j. The *interface* of the decomposition will include the closure of all the subdomain edges.

We remark the distinction between $S_{\mathcal{N}}^{\Omega_i}$ (nodes that are vertices of the polygonal subdomains) and $S_{\mathcal{V}}^{\Omega_i}$ (nodes that belong to at least three subdomains); see Figure 1. It is clear that $S_{\mathcal{V}}^{\Omega_i} \subset S_{\mathcal{N}}^{\Omega_i}$.

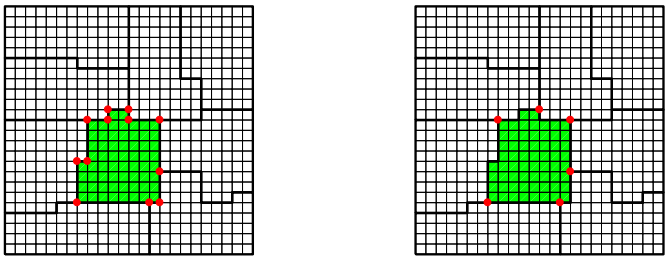

Fig. 1: A METIS decomposition for the unit square with square elements. The colored subdomain is a dodecagon with six subdomain edges. (a) Subdomain nodes, $S_{\mathcal{N}}^{\Omega_i}$ (left) (b) Subdomain vertices, $S_{\mathcal{V}}^{\Omega_i}$ (right)

We also define some polynomial spaces that will be used in the description of the algorithm. Given two non-negative integers α_1, α_2, we will use the standard notation for a multi-index $\boldsymbol{\alpha} = (\alpha_1, \alpha_2)$, with $|\boldsymbol{\alpha}| := \alpha_1 + \alpha_2$ and $\boldsymbol{x}^{\boldsymbol{\alpha}} := x_1^{\alpha_1} x_2^{\alpha_2}$ for any point in the plane $\boldsymbol{x} = (x_1, x_2)$. The space of polynomials of degree less than or equal to k defined on D will be denoted by $\mathcal{P}_k(D)$. We recall that $\dim \mathcal{P}_k(D) = (k+1)(k+2)/2$ for two-dimensional domains.

Let $m_{\boldsymbol{\alpha}}$ be the scaled monomial of degree $|\boldsymbol{\alpha}|$ in the domain D, defined by

$$m_{\boldsymbol{\alpha}}(\boldsymbol{x}) := \left(\frac{\boldsymbol{x} - \boldsymbol{x}_D}{h_D} \right)^{\boldsymbol{\alpha}},$$

where $\boldsymbol{x}_D$ is the barycenter of D and h_D its diameter. The set of such polynomials of degree less than or equal to k will be denoted by

$$\mathcal{M}_k(D) := \{ m_{\boldsymbol{\alpha}} : |\boldsymbol{\alpha}| \leq k \}. \tag{3}$$

Let D represent an element $K \in \mathcal{T}_h$ or a subdomain Ω_i. We distinguish between $\overline{v}_D$, the standard *nodal average* of v, and $\widehat{v}_D$, the *mean value* of v, defined respectively

by

$$\overline{v}_D := \frac{1}{|S_{\mathcal{N}}^D|} \sum_{\boldsymbol{x} \in S_{\mathcal{N}}^D} w(\boldsymbol{x}), \quad \text{and} \quad \widehat{v}_D := \frac{1}{|D|} \int_D w(\boldsymbol{x}) \, d\boldsymbol{x}.$$

For a positive integer k, we will also consider the set

$$\mathcal{B}_k(\partial D) := \{v \in C^0(\partial D) : v|_e \in \mathcal{P}_k(e) \ \forall \ e \subset \partial D\}$$

where e represents any edge on the boundary of D, and the local virtual element space

$$V_k^D := \{v \in H^1(D) : v \in \mathcal{B}_k(\partial D), \ \Delta v \in \mathcal{P}_{k-2}(D)\}. \tag{4}$$

We note that we consider $\mathcal{P}_{-1}(D) = 0$. Hence, a function in V_1^D is continuous and piecewise linear on the boundary of D and harmonic in the interior, and it is completely determined by its values at the nodes in $S_{\mathcal{N}}^D$.

Finally, we define the operator $\Pi_{D,k}^{\nabla} : V_k^D \to \mathcal{P}_k(D) \subset V_k^D$ where $\widetilde{v} := \Pi_{D,k}^{\nabla} v$ is the polynomial that satisfies

$$\begin{cases} a^D(\widetilde{v}, q) = a^D(v, q) & \forall \ q \in \mathcal{P}_k(D), \\ P_0(\widetilde{v}) = P_0(v). \end{cases} \tag{5}$$

Here, $P_0 : V_k^D \to \mathbb{R}$ is a projection operator onto constants, which is chosen as the nodal average if $k = 1$ or the mean value if $k \geq 2$; see Subsection 6.1 for implementation details related to the operator $\Pi_{D,k}^{\nabla}$.

3. Virtual Element Methods and discretization. We describe the basic theory of the VEM introduced in [1]; see also [2] for implementation details. We discretize (2) with the lowest-order VEM and we restrict in this section our presentation to this case. Nevertheless, for the approximation of the coarse space we will use the projectors $\Pi_{D,k}^{\nabla}$ for $k \geq 2$; see Subsection 4.2. It is assumed that the elements satisfy the following two assumptions, where h denotes the maximum of the diameters of the elements in $\mathcal{T}_h$:

ASSUMPTION 1. *There exists $\gamma > 0$ such that for all h, each element K in $\mathcal{T}_h$ is star-shaped with respect to a ball of radius greater than or equal to γh_K.*

ASSUMPTION 2. *There exists $\gamma > 0$ such that for all h and for each element K in $\mathcal{T}_h$, the distance between any two vertices of K is greater than or equal to γh_K.*

The global space of lowest-order virtual element functions is defined as

$$V_h := \{v \in H_0^1(\Omega) : v|_K \in V_1^K \ \forall \ K \in \mathcal{T}_h\},$$

where V_1^K is defined in (4). The dimension of V_h is equal to the number of nodes of $\mathcal{T}_h$ in the interior of Ω. It is easy to check that they are unisolvent ([1, Proposition 4.1]) and V_h reduces to the first-order Lagrange finite element space in the case of a triangular mesh.

We consider the canonical basis $\{\phi_{\boldsymbol{x}_i}^h\}$ of V_h such that, for any node $\boldsymbol{x}_j \in S_{\mathcal{N}}$, we have that $\phi_{\boldsymbol{x}_i}^h(\boldsymbol{x}_j) = \delta_{ij}$. For a continuous function u, we can define the natural interpolant onto V_h given by

$$I^h u := \sum_{\boldsymbol{x} \in S_{\mathcal{N}}} u(\boldsymbol{x}) \phi_{\boldsymbol{x}}^h.$$

We note that in general $a(\phi^h_{\boldsymbol{x}_i}, \phi^h_{\boldsymbol{x}_j})$ cannot be evaluated as discussed in [1, Section 4.5]. Therefore, we consider the local bilinear form $a_h^K : V_1^K \times V_1^K \to \mathbb{R}$ defined by

$$a_h^K(u,v) := a^K(\Pi^\nabla_{K,1}u, \Pi^\nabla_{K,1}v) + S^K(u - \Pi^\nabla_{K,1}u, v - \Pi^\nabla_{K,1}v), \tag{6}$$

where $S^K : V_1^K \times V_1^K \to \mathbb{R}$ is a stabilizing term, which can be chosen as

$$S^K(u,v) := \sum_{\boldsymbol{x} \in S^K_{\mathcal{N}}} \rho\ u(\boldsymbol{x})v(\boldsymbol{x}).$$

From (6) it is clear that a_h^K satisfies the consistency property

$$a_h^K(p,v) = a^K(p,v) \quad \forall\ p \in \mathcal{P}_1(K), \quad \forall\ v \in V_1^K,$$

and the stability property

$$\alpha_1 a^K(v,v) \le a_h^K(v,v) \le \alpha_2 a^K(v,v) \quad \forall\ v \in V_1^K, \tag{7}$$

where α_1, α_2 are independent of ρ, h_K and K; see [1, Theorem 4.1]. The discrete bilinear form and right hand side are then defined by

$$a_h(u,v) := \sum_{K \in \mathcal{T}_h} a_h^K(u,v), \quad F_h(v) := \sum_{K \in \mathcal{T}_h} |K| \widehat{f}\ \overline{v}.$$

Finally, the discrete formulation for problem (2) is: Find $u_h \in V_h$ such that

$$a_h(u_h, v_h) = F_h(v_h)\ \forall\ v_h \in V_h. \tag{8}$$

We refer to [1, 5] for an a priori estimate and approximation properties, [2] for implementation details and [17] for an implementation in Matlab.

4. Overlapping Schwarz methods. We briefly describe the two-level additive overlapping Schwarz methods; for a complete study see [18, Chapters 2, 3]. We also describe the *reduced virtual coarse space* V_0^R introduced in [6, Section 6] and the new operator R_0^T in detail.

4.1. The coarse space. Consider the partition $\mathcal{T}^H$ formed by the subdomains $\{\Omega_i\}_{i=1}^N$. For each subdomain, let $V_1^i := V_1^{\Omega_i}$ be the lowest-order local virtual space defined in (4). The degrees of freedom are chosen again as the values at the nodes in $S^{\Omega_i}_{\mathcal{N}}$. Then, the global virtual space on $\mathcal{T}^H$ is defined as

$$V_0 := \left\{ v \in H_0^1(\Omega) : v|_{\Omega_i} \in V_1^i,\ 1 \le i \le N \right\}.$$

For each subdomain vertex $\boldsymbol{x}_0 \in S_{\mathcal{V}}$ we define a coarse function $\psi^H_{\boldsymbol{x}_0} \in V_0$ by choosing appropriately its degrees of freedom. First, we set $\psi^H_{\boldsymbol{x}_0}(\boldsymbol{x}) = 0$ for all the subdomain vertices $\boldsymbol{x}$, except at $\boldsymbol{x}_0$ where $\psi^H_{\boldsymbol{x}_0}(\boldsymbol{x}_0) = 1$. Second, we set the degrees of freedom related to the nodal values on each subdomain edge. If $\boldsymbol{x}_0$ is not an endpoint of $\mathcal{E}$, then $\psi^H_{\boldsymbol{x}_0}$ vanishes on that edge. If $\mathcal{E}$ has endpoints $\boldsymbol{x}_0$ and $\boldsymbol{x}_1$, let $\boldsymbol{d}_{\mathcal{E}}$ be the unit vector with direction from $\boldsymbol{x}_1$ to $\boldsymbol{x}_0$. Consider any node $\widetilde{\boldsymbol{x}} \in \mathcal{E}$. If $0 \le (\widetilde{\boldsymbol{x}} - \boldsymbol{x}_1) \cdot \boldsymbol{d}_{\mathcal{E}} \le |\boldsymbol{x}_0 - \boldsymbol{x}_1|$, we then set

$$\psi^H_{\boldsymbol{x}_0}(\widetilde{\boldsymbol{x}}) = \frac{(\widetilde{\boldsymbol{x}} - \boldsymbol{x}_1) \cdot \boldsymbol{d}_{\mathcal{E}}}{|\boldsymbol{x}_0 - \boldsymbol{x}_1|}. \tag{9}$$

It is clear that $\psi^H_{\boldsymbol{x}_0}(\boldsymbol{x}_0) = 1$, $\psi^H_{\boldsymbol{x}_0}(\boldsymbol{x}_1) = 0$ and that the function varies linearly in the direction of $\boldsymbol{d}_{\mathcal{E}}$ for such nodes. If $(\widetilde{\boldsymbol{x}} - \boldsymbol{x}_1)\cdot\boldsymbol{d}_{\mathcal{E}} < 0$ or $(\widetilde{\boldsymbol{x}} - \boldsymbol{x}_1)\cdot\boldsymbol{d}_{\mathcal{E}} > |\boldsymbol{x}_0 - \boldsymbol{x}_1|$, we then set $\psi^H_{\boldsymbol{x}_0}(\widetilde{\boldsymbol{x}}) = 0$ or $\psi^H_{\boldsymbol{x}_0}(\widetilde{\boldsymbol{x}}) = 1$, respectively. In this way, we define all the degrees of freedom of $\psi^H_{\boldsymbol{x}_0} \in V_0$. By construction it is clear that $0 \le \psi^H_{\boldsymbol{x}_0} \le 1$ and the sum $\sum_{\boldsymbol{x}_0}\psi^H_{\boldsymbol{x}_0}$ of all these coarse basis functions is equal to one.

We then define the *reduced coarse space* as the span of $\{\psi^H_{\boldsymbol{x}_0}\}$, i.e.,

$$V_0^R := \Big\{ v \in H^1_0(\Omega) : v = \sum_{\boldsymbol{x}_0 \in S_{\mathcal{V}}} \alpha_{\boldsymbol{x}_0}\psi^H_{\boldsymbol{x}_0} \Big\} \subset V_0,$$

where $\alpha_{\boldsymbol{x}_0} \in \mathbb{R}\ \forall\ \boldsymbol{x}_0 \in S_{\mathcal{V}}$. We note that there is only one degree of freedom per subdomain vertex, and that functions are piecewise linear on the subdomain edges and harmonic in the interior of each subdomain. We can naturally define a linear interpolant $I^H : V_h \to V_0^R$ by

$$I^H u := \sum_{\boldsymbol{x}_0 \in S_{\mathcal{V}}} u(\boldsymbol{x}_0)\psi^H_{\boldsymbol{x}_0},$$

and it is easy to deduce that I^H reproduces linear polynomials.

4.2. Extension operators. The crucial aspect in the construction of the preconditioner is to define an operator $R_0^T : V_0^R \to V_h$ that approximates functions in the coarse space by elements in V_h. The straightforward approach would be to evaluate each coarse basis function $\psi^H_{\boldsymbol{x}_0}$ at the internal nodes of the subdomains, but these coarse functions are virtual and we only know the value of their degrees of freedom. We could consider also the discrete harmonic extension for each subdomain Ω_i by using the bilinear form $a(\cdot,\cdot)$ restricted to Ω_i. This is the usual approach in most of the existing literature; see, e.g., [8, 7, 16, 19, 9]. A different approach is presented in [6], where R_0^T is constructed by considering piecewise-linear contributions.

Instead, we take advantage of the operators $\Pi^{\nabla}_{\Omega_i,k}$ defined in (5). We start by describing the virtual space when $k \ge 2$. For each subdomain Ω_i, the local virtual space of degree k is defined by $V_k^i := V_k^{\Omega_i}$; see (4). It is easy to deduce that $\dim V_k^i = n_i k + k(k-1)/2$, where n_i is the number of edges of the polygon Ω_i. The degrees of freedom of a function $v \in V_k^i$ can be chosen as:

(a) The values of v at the n_i vertices of the polygon Ω_i.
(b) The values of v at $k-1$ internal points of each edge of Ω_i.
(c) The moments $\dfrac{1}{|\Omega_i|}\displaystyle\int_{\Omega_i} m(\boldsymbol{x})v(\boldsymbol{x})\ d\boldsymbol{x} \quad \forall\ m \in \mathcal{M}_{k-2}(\Omega_i)$, where $\mathcal{M}_{k-2}$ is the set of scaled monomials defined in (3).

Then, the global virtual space on $\mathcal{T}^H$ of degree k is defined as

$$V_H^k := \left\{ v \in H^1_0(\Omega) : v|_{\Omega_i} \in V_k^i,\ 1 \le i \le N \right\}.$$

Clearly $V_0^R \subset V_0 \subset V_H^k$. Thus, given a coarse basis function $\psi^H_{\boldsymbol{x}_0}$, we can identify it as an element of V_H^k by computing its degrees of freedom (a), (b) and (c). We note that the nodal degrees of freedom given in (a) and (b) are straightforward to compute by using (9). We then need to compute the moments (c), namely

$$|\Omega_i|^{-1}\int_{\Omega_i} m_{\boldsymbol{\alpha}}(\boldsymbol{x})\psi^H_{\boldsymbol{x}_0}(\boldsymbol{x})\ d\boldsymbol{x}, \quad \forall\ m_{\boldsymbol{\alpha}} \in \mathcal{M}_{k-2}(\Omega_i),$$

which might seem difficult. However, we recall that $\psi^H_{\boldsymbol{x}_0}$ is harmonic in Ω_i. Thus, it is enough to choose these moments in such way that $a^{\Omega_i}(\psi^H_{\boldsymbol{x}_0}, \psi^H_{\boldsymbol{x}_0})$ is minimized among

all the functions in V_H^k with the prescribed boundary data. As we will show, this is equivalent to solving a linear system with $k(k-1)/2$ unknowns for each subdomain Ω_i; see Subsection 6.1 for implementation details.

We then define the action of R_0^T on each basis function of V_0^R. We note that R_0^T depends on $k \geq 2$, but for simplicity we omit this dependence. We set the degrees of freedom of $R_0^T \psi_{\boldsymbol{x}_0}^H \in V_h$ as follows:

(a') If $\boldsymbol{x}$ is a node of $\mathcal{T}_h$ in the interior of Ω_i, we set

$$(R_0^T \psi_{\boldsymbol{x}_0}^H)(\boldsymbol{x}) := (\Pi_{\Omega_i,k}^{\nabla} \psi_{\boldsymbol{x}_0}^H)(\boldsymbol{x}).$$

(b') For all the other nodes in $\mathcal{T}_h$ (that belong to the interface), we set

$$(R_0^T \psi_{\boldsymbol{x}_0}^H)(\boldsymbol{x}) := \psi_{\boldsymbol{x}_0}^H(\boldsymbol{x}).$$

Therefore, given $u_0 = \sum_{\boldsymbol{x} \in S_{\mathcal{V}}} \alpha_{\boldsymbol{x}} \psi_{\boldsymbol{x}}^H \in V_0^R$, we can write the restriction of R_0^T to a subdomain Ω_i as

$$(R_0^T u_0)|_{\Omega_i} = I^h \left(\Pi_{\Omega_i,k}^{\nabla} u_0 \right) + \sum_{\boldsymbol{x} \in S_{\mathcal{N}} \cap \partial\Omega_i} (u_0 - \Pi_{\Omega_i,k}^{\nabla} u_0)(\boldsymbol{x}) \phi_{\boldsymbol{x}}^h. \tag{10}$$

Finally, we consider the bilinear form defined in $V_0^R \times V_0^R$ by

$$\tilde{a}_{h,0}(u_0, v_0) := a_h(R_0^T u_0, R_0^T v_0) = \sum_{K \in \mathcal{T}_h} a_h^K (R_0^T u_0, R_0^T v_0). \tag{11}$$

We note that as we increase k, the possibility of choosing more moments (c) allows us to obtain a better approximation $R_0^T \psi_{\boldsymbol{x}}^H$ for $\psi_{\boldsymbol{x}}^H$ by just solving a small linear system. In practice, results for $k = 2$ and $k = 3$ are quite competitive as it is shown in Section 6.

4.3. Local spaces. We consider the usual local virtual spaces V_i, $1 \leq i \leq N$, defined by

$$V_i := \left\{ v \in H_0^1(\Omega_i') : v|_K \in \mathcal{B}_1(\partial K),\ \Delta v|_K = 0 \text{ in } K,\ \forall\, K \subset \Omega_i' \right\}.$$

Thus, the degrees of freedom are the values at the nodes of $\mathcal{T}_h$ in the interior of Ω_i'. We also consider the natural operators $R_i^T : V_i \to V_h$ given by the zero extension from the subdomain Ω_i' to Ω, $1 \leq i \leq N$. We use exact solvers for the local spaces, i.e., we define the bilinear forms $\tilde{a}_{h,i} : V_i \times V_i \to \mathbb{R}$ given by

$$\tilde{a}_{h,i}(u_i, v_i) := a_h(R_i^T u_i, R_i^T v_i) = \sum_{K \in \Omega_i'} a_h^K(u_i, v_i), \quad 1 \leq i \leq N. \tag{12}$$

4.4. Algorithm. In this subsection we define an additive preconditioner for the ill-conditioned sparse linear system $A\boldsymbol{\lambda} = \boldsymbol{g}$ obtained from problem (8), where $A_{i,j} = a_h(\phi_{\boldsymbol{x}_j}^h, \phi_{\boldsymbol{x}_i}^h)$, $\boldsymbol{g}_i = F_h(\phi_{\boldsymbol{x}_i}^h)$ and $\boldsymbol{\lambda}$ is the vector of coordinates of the solution with respect to the basis $\{\phi_{\boldsymbol{x}_i}^h\}$ of V_h, i.e., $u_h = \sum \lambda_i \phi_{\boldsymbol{x}_i}^h$.

Consider the matrix representation of the operators R_i^T denoted again by R_i^T. We define the stiffness matrices $\tilde{A}_i = R_i A R_i^T$, $0 \leq i \leq N$, and then consider the Schwarz projections $P_i = R_i^T \tilde{A}_i^{-1} R_i A$, $0 \leq i \leq N$. The additive preconditioned operator is defined by

$$P_{ad} := \sum_{i=0}^{N} P_i = A_{ad}^{-1} A, \text{ with } A_{ad}^{-1} = \sum_{i=0}^{N} R_i^T \tilde{A}_i^{-1} R_i. \tag{13}$$

Multiplicative and hybrid preconditioners can be considered as well; see [18, Section 2.2]. For the preconditioned system $A_{ad}^{-1}A\boldsymbol{\lambda} = A_{ad}^{-1}\boldsymbol{g}$, we have the main theorem of this paper. Its proof is presented in Section 5.

THEOREM 4.1. *There exists a constant C, independent of H, h and ρ, such that the condition number of the preconditioned system $\kappa(A_{ad}^{-1}A)$ satisfies*

$$\kappa(A_{ad}^{-1}A) \leq C\left(1+\log\frac{H}{h}\right)\left(1+\frac{H}{\delta}\right),$$

where the ratios H/h and H/δ denote their maximum value over all the subdomains.

5. Technical Tools. We collect some tools that are needed in the proof of Theorem 4.1. For simplicity we write $\omega_i := 1+\log(H_i/h_i)$ and $\omega := \max_i \omega_i$. We recall the following Poincaré and discrete Sobolev inequalities:

LEMMA 5.1. *Let Ω be Lipschitz continuous with diameter H. Then, there exists a constant C that depends only on the shape of Ω but not on H, such that*

$$\|u\|^2_{L^2(\Omega)} \leq CH^2|u|^2_{H^1(\Omega)},$$

for $u \in H^1(\Omega)$ with vanishing mean value.

Proof. See [18, Corollary A.15]. ∎

LEMMA 5.2. *Given $v \in V_h$ with zero mean value, there exists a constant C such that*

$$\|v\|^2_{L^\infty(\Omega_i)} \leq C\omega_i|v|^2_{H^1(\Omega_i)},$$

where C is independent of H_i and h_i.

Proof. See [3], [4, Section 4.9] for a proof with domains satisfying an interior cone condition. This inequality holds for more general subdomains; see, e.g., [7, Lemma 3.2] for a proof with John domains. ∎

We then have the following estimates for the interpolation operators I^h and $\Pi^{\nabla}_{\Omega_i,k}$:

LEMMA 5.3. *Let $K \in \mathcal{T}_h$ and $v \in H^2(K)$. Then, there exists C, independent of h_K, such that*

$$|v - I^h v|_{H^s(K)} \leq Ch_K^{2-s}|v|_{H^2(K)},$$

with $s \in \{0,1\}$.

Proof. See [5, Lemma 3.3.4]. ∎

LEMMA 5.4. *Let $K \in \mathcal{T}_h$ and suppose that there exists a triangular partition $\mathcal{T}_K$ of K such that $u \in H^1(\Omega)$ is a quadratic function in each $T \in \mathcal{T}_K$. Then, there exists a constant C such that*

$$|I^h u|_{H^1(K)} \leq C|u|_{H^1(K)},$$

where C is independent of h_K.

Proof. This is a modification of [18, Lemma 3.9]; see the details in [6, Lemma 4.6]. ∎

LEMMA 5.5. *Given $k \geq 2$ and $u_0 \in V_k^i$, there exists a constant C such that*

$$|\Pi^{\nabla}_{\Omega_i,k} u_0|^2_{H^1(\Omega_i)} \leq |u_0|^2_{H^1(\Omega_i)},$$
$$\|u_0 - \Pi^{\nabla}_{\Omega_i,k} u_0\|^2_{L^2(\Omega_i)} \leq C H_i^2 |u_0|^2_{H^1(\Omega_i)},$$

where C is independent of H_i.

Proof. Let $\widetilde{u}_0 := \Pi^{\nabla}_{\Omega_i,k} u_0 \in \mathcal{P}_k(\Omega_i)$. The first inequality follows straightforward from the definition of $\Pi^{\nabla}_{\Omega_i,k}$, since $a^{\Omega_i}(u_0 - \widetilde{u}_0, u_0 - \widetilde{u}_0) \geq 0$ and $a^{\Omega_i}(u_0 - \widetilde{u}_0, \widetilde{u}_0) = 0$. The second inequality is a consequence of Lemma 5.1, since u_0 and $\widetilde{u}_0$ have the same mean value over Ω_i by definition of the operator for $k \geq 2$. ∎

We now obtain some bounds for the operators introduced in Section 4:

LEMMA 5.6. *Given $u \in V_h$, let $u_0 := I^H u \in V_0^R$. Then, there exists a constant C such that*

$$|u_0|^2_{H^1(\Omega_i)} \leq C \omega_i |u|^2_{H^1(\Omega_i)},$$

where C is independent of H_i and h_i.

Proof. See [6, Lemma 4.4 and Theorem 6.1]. ∎

LEMMA 5.7. *Given $u \in V_h$, let $u_0 := I^H u \in V_0^R$. If $k \geq 2$, then there exists a constant C such that*

$$\|u - R_0^T u_0\|^2_{L^2(\Omega_i)} \leq C H_i^2 \omega_i |u|^2_{H^1(\Omega_i)},$$
$$|R_0^T u_0|^2_{H^1(\Omega_i)} \leq C w_i |u|^2_{H^1(\Omega_i)},$$

where C is independent of H_i and h_i.

Proof. Define $\widetilde{u}_0 := \Pi^{\nabla}_{\Omega_i,k} u_0$. By triangle inequality and (10), we have that

$$\|u - R_0^T u_0\|^2_{L^2(\Omega_i)} \leq 5\Big(\|u - \widehat{u}\|^2_{L^2(\Omega_i)} + \|u_0 - \widehat{u}\|^2_{L^2(\Omega_i)} + \|\widetilde{u}_0 - u_0\|^2_{L^2(\Omega_i)} + \|I^h \widetilde{u}_0 - \widetilde{u}_0\|^2_{L^2(\Omega_i)} + \|g\|^2_{L^2(\Omega_i)}\Big),$$

where $\widehat{u}$ is the mean value of u over Ω_i and

$$g := \sum_{\boldsymbol{x} \in S_{\mathcal{N}} \cap \partial\Omega_i} (u_0 - \widetilde{u}_0)(\boldsymbol{x}) \phi^h_{\boldsymbol{x}} \in V_h.$$

We bound each term of the last sum separately. The first term is easily bounded by Lemma 5.1. In turn, for the second term we have that

$$\|u_0 - \widehat{u}\|^2_{L^2(\Omega_i)} = \|I^H(u - \widehat{u})\|^2_{L^2(\Omega_i)} \leq C H_i^2 \|u - \widehat{u}\|^2_{L^\infty(\Omega_i)},$$

and we use then Lemma 5.2 to obtain the required bound. Here, we have used that $I^H(u - \widehat{u})$ is harmonic in Ω_i and that the values (9) are uniformly bounded. For the third term, we recall that $u_0 - \widetilde{u}_0$ has zero mean value. Thus,

$$\|\widetilde{u}_0 - u_0\|^2_{L^2(\Omega_i)} \leq C H_i^2 |\widetilde{u}_0 - u_0|^2_{H^1(\Omega_i)},$$

and we then use Lemma 5.5 and Lemma 5.6.

Next, the fourth term is bounded by using Lemma 5.3, an inverse inequality for polynomials, Lemma 5.5 and Lemma 5.6. Finally, we note that g vanishes on all the elements K that do not intersect $\partial\Omega_i$. For the remaining elements,

$$\|g\|^2_{L^2(K)} \leq Ch_K^2 \|u_0 - \widetilde{u}_0\|^2_{L^\infty(\Omega_i)} \leq Ch_K^2 |\widetilde{u}_0 - u_0|^2_{H^1(\Omega_i)}.$$

By adding all the contributions, we get

$$\|g\|^2_{L^2(\Omega_i)} \leq CH_i^2 |\widetilde{u}_0 - u_0|^2_{H^1(\Omega_i)},$$

and we conclude by using Lemma 5.5 and Lemma 5.6.

In order to deduce the second inequality, by Lemma 5.5 and Lemma 5.6 we note that it is enough to bound the H^1-seminorm of $R_0^T u_0 - \widetilde{u}_0$. We have that

$$|R_0^T u_0 - \widetilde{u}_0|^2_{H^1(\Omega_i)} \leq |I^h \widetilde{u}_0 - \widetilde{u}_0|^2_{H^1(\Omega_i)} + |g|^2_{H^1(\Omega_i)}.$$

The first term is easily bounded by $|\widetilde{u}_0|^2_{H^1(\Omega_i)}$, where we use Lemma 5.3 and an inverse inequality for polynomials. Finally, since the energy of each basis function $\phi^h_{\boldsymbol{x}}$ is uniformly bounded, for an element with an edge on $\partial\Omega_i$ we have that

$$\begin{aligned} |g|^2_{H^1(K)} &\leq Ch_K^{-1} \|u_0 - \widetilde{u}_0\|^2_{L^2(\partial K)} \\ &\leq Ch_K^{-1} \|u_0 - \widetilde{u}_0\|_{L^2(K)} \|u_0 - \widetilde{u}_0\|_{H^1(K)} \\ &\leq C \|u_0 - \widetilde{u}_0\|^2_{H^1(K)}, \end{aligned}$$

where we have used a standard trace estimate; see, e.g., [4, Theorem 1.6.6]. We then add all the contributions and use Lemma 5.1, Lemma 5.5 and Lemma 5.6 to conclude the proof of our lemma. ∎

We now present the proof of our main theorem:

Proof. (Theorem 4.1) Given $u \in V_h$, we define

$$u_0 := I^H u \in V_0^R \quad \text{and} \quad u_i := R_i(I^h(\tilde{\theta}_i(u - R_0^T u_0))) \in V_i,$$

with $\tilde{\theta}_i$ a typical partition of unity for the overlapping subdomains Ω_i'; see [18, Lemma 3.4]. It is straightforward to verify that $\sum_{i=0}^N R_i^T u_i = u$. By [18, Theorem 3.13], if there exists a constant C_0 such that

$$\sum_{i=0}^N \tilde{a}_{h,i}(u_i, u_i) \leq C_0^2 \; a_h(u,u), \tag{14}$$

then it holds that $\kappa(P_{ad}) \leq (N^C + 1)C_0^2$, where N^C is the minimum number of colors needed to paint the overlapping subdomains Ω_i' such that no pair of subdomains of the same color intersect.

For the sake of completeness we present the main ideas required to estimate C_0; we refer to [6, Theorem 3.1] for more details. From (11), (7) and Lemma 5.7 it is easy to deduce that

$$\tilde{a}_{h,0}(u_0, u_0) \leq C \frac{\alpha_2}{\alpha_1} \omega a_h(u,u). \tag{15}$$

For any element $K \in \mathcal{T}_h$, we consider a fixed triangular mesh $\mathcal{T}_K$ of K. Denote by I_K the piecewise-linear interpolant onto $\mathcal{T}_K$. Define then θ_i^ℓ, $w^\ell \in H^1(\Omega_i)$ element by element by

$$\theta_i^\ell|_K := I_K \tilde{\theta}_i \text{ and } \; w^\ell|_K := I_K(u - R_0^T u_0).$$

It is clear that θ_i^ℓ satisfies $\|\nabla\theta_i^\ell\|_{L^\infty(K)} \leq \|\nabla\tilde{\theta}_i\|_{L^\infty(K)} \leq C/\delta_i$. From (12), (7) and Lemma 5.4 we deduce that

$$\tilde{a}_{h,i}(u_i,u_i) \leq C\alpha_2 \left(\int_{\Omega_i'} \rho|\theta_i^\ell \nabla w^\ell|^2 \, d\boldsymbol{x} + \int_{\Omega_i'} \rho|w^\ell \nabla\theta_i^\ell|^2 \, d\boldsymbol{x} \right). \tag{16}$$

We have that $|w^\ell|^2_{H^1(K)} \leq C\|u - R_0^T u_0\|^2_{H^1(K)}$ by using an inverse inequality. Since $|\theta_i^\ell| \leq 1$, the first term in the sum of (16) can be bounded then by

$$\int_{\Omega_i'} \rho \, |\theta_i^\ell \nabla w^\ell|^2 \, d\boldsymbol{x} \leq C \sum_{j\in\Xi_i} \rho_j \|u - R_0^T u_0\|^2_{H^1(\Omega_j)} \leq C\omega \sum_{j\in\Xi_i} a^{\Omega_j}(u,u), \tag{17}$$

where we have used Lemma 5.7. Here, $\Xi_i := \{j : \overline{\Omega}_j \cap \overline{\Omega}_i \neq \emptyset\}$.

In order to estimate the last term in (16), we note that the gradient of θ_i^ℓ is not zero only in a neighborhood of $\partial\Omega_i$ of width $\max_{j\in\Xi_i}\delta_j$. The number of sets Ω_j' that intersect Ω_i is uniformly bounded, and therefore we need to consider the contribution from only one of them. We write $w^\ell = w_1^\ell + w_2^\ell$, with $w_1^\ell|_K := I_K(u - u_0)$ and $w_2^\ell|_K := I_K(u_0 - R_0^T u_0)$ for each element K.

Since $\|w_1^\ell\|_{L^\infty(\Omega_i)} \leq C\|u - \widehat{u}\|_{L^\infty(\Omega_i)}$, we have that

$$\int_{\Omega_j'\cap\Omega_i} \rho_i \, |w_1^\ell \nabla\theta_i^\ell|^2 \, d\boldsymbol{x} \leq C \, \frac{\rho_i}{\delta_i^2} \, \|u - \widehat{u}\|^2_{L^\infty(\Omega_i)} |\Omega_j' \cap \Omega_i| \leq C \, \frac{H_i}{\delta_i} \, \omega_i a^{\Omega_i}(u,u). \tag{18}$$

For the remaining term w_2^ℓ, we cover $\Omega_j' \cap \Omega_i$ with square patches with sides on the order of δ_i and note that on the order of H_i/δ_i of them will suffice. For a square π_k we can bound

$$\int_{\pi_k} \rho_i |w_2^\ell \nabla\theta_i^\ell|^2 \, d\boldsymbol{x} \leq \frac{C}{\delta_i^2}\rho_i \, \|w_2^\ell\|^2_{L^2(\pi_k)} \leq C\rho_i |w_2^\ell|^2_{H^1(\pi_k)}$$

where we have used a Friedrich's inequality, since w_2^ℓ vanishes on $\partial\Omega_i$. By adding all the contributions from the squares π_k we can conclude that

$$\int_{\Omega_i'} \rho|w^\ell \nabla\theta_i^\ell|^2 \, d\boldsymbol{x} \leq C \, \left(1 + \frac{H}{\delta}\right) \, \omega \sum_{j\in\Xi_i} a^{\Omega_j}(u,u). \tag{19}$$

Thus, by substituting (17) and (19) in (16), we obtain

$$\tilde{a}_{h,i}(u_i,u_i) \leq C\frac{\alpha_2}{\alpha_1} \, \omega \left(1 + \frac{H}{\delta}\right) \sum_{j\in\Xi_i} \sum_{K\subset\Omega_j} a_h^K(u,u). \tag{20}$$

From (15) and (20) we conclude that (14) holds with

$$C_0^2 := C\frac{\alpha_2}{\alpha_1} \left(1 + \frac{H}{\delta}\right) \left(1 + \log\frac{H}{h}\right),$$

and our proof is complete. ∎

6. Experimental results. In this section we discuss some implementation details and present numerical results for our two-level overlapping additive algorithm with $\Omega = [0,1]^2$.

6.1. Implementation. We first describe how to compute the operators $\Pi^{\nabla}_{\Omega_i,k}$; see [2] for more details. Consider a subdomain Ω_i and the basis of scaled monomials $\mathcal{M}_{k-2}(\Omega_i)$. We use the natural ordering for the multi-indices

$$\boldsymbol{\alpha}_1 = (0,0), \boldsymbol{\alpha}_2 = (1,0), \boldsymbol{\alpha}_3 = (0,1), \ldots, \boldsymbol{\alpha}_{N_{\mathcal{M}}} = (0, k-2),$$

with $N_{\mathcal{M}} := k(k-1)/2$ the dimension of $\mathcal{M}_{k-2}$. We also order the degrees of freedom of V_k^i and denote by $dof_p(u)$ the functional that computes the *p-th* degree of freedom of a given function u, $1 \leq p \leq N_{\mathcal{V}}$, with $N_{\mathcal{V}} := \dim V_k^i$. In this way, we define the canonical basis $\{\varphi_p\}$ of V_k^i such that $dof_p(\varphi_q) = \delta_{pq}$. We then define the $N_{\mathcal{V}} \times N_{\mathcal{M}}$ matrix D, where its entries are given by

$$D_{pj} = dof_p(m_{\boldsymbol{\alpha}_j}),$$

and the $N_{\mathcal{M}} \times N_{\mathcal{V}}$ matrix B given by

$$B := \begin{bmatrix} P_0\varphi_1 & \cdots & P_0\varphi_{N_{\mathcal{V}}} \\ (\nabla m_{\boldsymbol{\alpha}_2}, \nabla\varphi_1)_{0,\Omega_i} & \cdots & (\nabla m_{\boldsymbol{\alpha}_2}, \nabla\varphi_{N_{\mathcal{V}}})_{0,\Omega_i} \\ \vdots & \ddots & \vdots \\ (\nabla m_{\boldsymbol{\alpha}_{N_{\mathcal{M}}}}, \nabla\varphi_1)_{0,\Omega_i} & \cdots & (\nabla m_{\boldsymbol{\alpha}_{N_{\mathcal{M}}}}, \nabla\varphi_{N_{\mathcal{V}}})_{0,\Omega_i} \end{bmatrix}.$$

By simple linear algebra, it is easy to show that the matrix representation of the operator $\Pi^{\nabla}_{\Omega_i,k}$ acting from V_k^i to $P_k(\Omega_i)$ in the basis $\mathcal{M}_k(\Omega_i)$ is given by

$$\Pi^{\nabla}_* := (BD)^{-1}D.$$

We can compute B by using the formula

$$\int_{\Omega_i} \nabla m_{\boldsymbol{\alpha}} \cdot \nabla\varphi_p \, d\boldsymbol{x} = -\int_{\Omega_i} \varphi_p \Delta m_{\boldsymbol{\alpha}} \, d\boldsymbol{x} \; + \int_{\partial\Omega_i} \varphi_p \frac{\partial m_{\boldsymbol{\alpha}}}{\partial \boldsymbol{n}} \, d\boldsymbol{s}.$$

The first integral in the sum can be computed with the moments of φ_p since $\Delta m_{\boldsymbol{\alpha}} \in \mathcal{P}_{k-2}$. For the last integral, φ_p is a polynomial on the boundary of the subdomain. Thus, the entries of B can be computed exactly up to machine precision.

Next, we describe how to compute the matrix R_0^T. We note that there is one column for each coarse basis function. Given a subdomain vertex $\boldsymbol{x}_0$, its column contains the values of the degrees of freedom of $R_0^T\psi^H_{\boldsymbol{x}_0}$ in V_h. The values of $\psi^H_{\boldsymbol{x}_0}$ at the nodes on the interface are computed from the definition of $\psi^H_{\boldsymbol{x}_0}$. For the interior nodes of a subdomain Ω_i, we compute the degrees of freedom as follows. Consider the local matrix $A^{(i)}$ written in block form

$$A^{(i)} = \begin{bmatrix} A^{(i)}_{II} & A^{(i)}_{IB} \\ A^{(i)}_{BI} & A^{(i)}_{BB} \end{bmatrix}$$

where I and B stand for interior and boundary degrees of freedom, respectively. Similarly, we write the projector matrix Π^{∇}_* in block form

$$\Pi^{\nabla}_* = [\Pi_{*,1}, \Pi_{*,2}],$$

where the first block $\Pi_{*,1}$ includes the columns related to the nodal degrees of freedom, and the second block $\Pi_{*,2}$ has the columns related to the degrees of freedom for the moments. Similarly, we write the degrees of freedom of $\psi^H_{\boldsymbol{x}_0}$ as a column vector

$[D_1, D_2]^T$, with D_2 the unknown moments. Therefore, the coefficients of the polynomial $\Pi^{\nabla}_{\Omega_i,k}\psi^H_{\boldsymbol{x}_0}$ on the scaled monomial basis $\mathcal{M}_k(\Omega_i)$ are given by $\Pi^{\nabla}_{*}[D_1, D_2]^T$. If we denote by M the matrix whose columns are the scaled monomials evaluated at the interior nodes of Ω_i and by v_B the values of $\psi^H_{\boldsymbol{x}_0}$ at the nodes of $\mathcal{T}_h$ on $\partial\Omega_i$, when finding the minimum of $a^{\Omega_i}(\psi^H_{\boldsymbol{x}_0}, \psi^H_{\boldsymbol{x}_0})$ we obtain the linear system with $k(k-1)/2$ unknowns given by

$$(\Pi^T_{*,2} M^T A^{(i)}_{II} M \Pi_{*,2}) D_2 = -(v_B^T A^{(i)}_{BI} M \Pi_{*,2} + \Pi^T_{*,2} M^T A^{(i)}_{II} M \Pi_{*,1} D_1).$$

After solving for D_2, the degrees of freedom inside the subdomain are given by

$$M\left(\Pi_{*,1} D_1 + \Pi_{*,2} D_2\right).$$

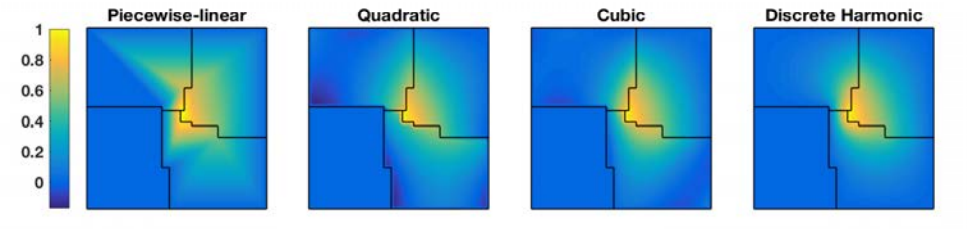

Fig. 2: Different approximations for a coarse basis function with square elements and METIS subdomains ($\rho = 1$).

We show the time required to assemble the matrix R_0^T as a function of H/h in Figure 3 for different approaches. We consider the case of discrete harmonic extensions as considered in [9], the case of piecewise-linear approximations studied in [6] and our operator R_0^T for $k = 2$ and $k = 3$. The assembling times are obtained by a serial code implemented in Matlab. For simplicity, we consider square elements and just four METIS subdomains. The computed time includes the factorization of the local matrices in the case of discrete harmonic extensions, and the computation of the local projectors Π^{∇}_{*} for our method. In all the cases, the values on the interface are computed similarly.

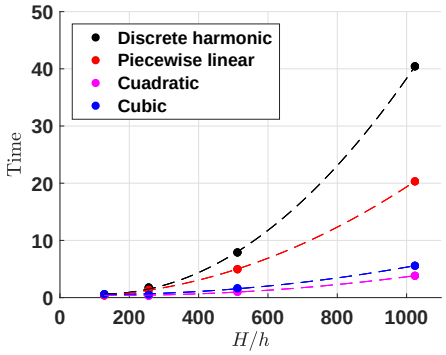

Fig. 3: Assembling time (in seconds) for R_0^T.

6.2. Examples. We present some experiments to verify the bound obtained in Theorem 4.1. We consider different polygonal meshes with square and irregular subdomains (created with the mesh-partitioner software METIS [15]); see Figure 4 for a triangulation with hexagons and irregular polygons. We estimate the condition number κ and compute the number of iterations I_2 (for $k = 2$), I_3 (for $k = 3$) and $I_{\mathcal{H}}$ (for the coarse space [9] based on discrete harmonic extensions) for each experiment. We note that our operator R_0^T recovers the bilinear Q_1 coarse space if Ω_i is a square and for this reason we only compute I_2 when considering square subdomains. For METIS subdomains we compare the different approximations.

Fig. 4: Solution with virtual elements for hexagonal (left) and irregular (right) meshes and constant coefficient $\rho = 1$.

We solve the resulting linear systems using the preconditioned conjugate gradient method to a relative residual tolerance of 10^{-6}. We compute the right-hand side such that the exact solution is $u(x_1, x_2) = \sin(\pi x_1)\sin(\pi x_2)$ when $\rho = 1$. When referring to discontinuous coefficients, we generate random numbers $r_i \in [-3, 3]$ with a uniform distribution and assign $\rho_i = 10^{r_i}$ to each individual element inside Ω_i.

6.2.1. Triangular mesh. For this case, the VEM corresponds to the first-order Lagrange space P_1 and our analysis provides a new approximation for the coarse space when using irregular subdomains. We verify that our algorithm is scalable and observe the logarithmic factor when ρ is discontinuous across the interface; see results in Table 1. We also confirm the linear growth in the condition number as we increase H/δ; see Figure 5.

6.2.2. Square mesh. For this case we present two sets of results. First, we discretize problem (2) with the Q_1 standard space of bilinear elements in order to compare our results to the ones in [9]; see Table 2. In this setting, our coarse space provides a new approach for irregular subdomains. Second, we solve the discrete problem (8) obtained by VEM; see Table 3. In the latter case, results are essentially the same when $\rho = 1$ and we omit them. We also verify the linear dependence on H/δ in both cases; see Figure 6.

6.2.3. Hexagonal and irregular polygons. For this set of examples we consider polygonal triangulations with METIS subdomains as in Figure 4. The irregular mesh is obtained from a Voronoi diagram for a given set of random numbers in the unit square and contains polygons with different number of edges. We solve the linear system that arises from Equation (8) and we note that results are quite similar if we use discrete harmonic extensions or our spaces even for $k = 2$. We confirm the scalability in Table 4; see also Table 5 and Figure 7 for the dependence on H/h and

Table 1: Number of iterations I and condition number κ (in parenthesis) for our problem with triangular elements and N subdomains. I_2, I_3 and $I_{\mathcal{H}}$ correspond to $k = 2$, $k = 3$ and discrete harmonic extensions, respectively. N_V is the dimension of the coarse space.

	Square subd		METIS subdomains			
	N_V	$I_2\,(\kappa)$	N_V	$I_2\,(\kappa)$	$I_3\,(\kappa)$	$I_{\mathcal{H}}\,(\kappa)$
N	Test 1: $H/h = 16$, $H/\delta = 4$, $\rho = 1$					
12^2	121	14 (6.0)	243	26 (10.3)	26 (10.2)	25 (9.8)
16^2	225	14 (5.9)	447	27 (12.9)	26 (12.2)	26 (12.2)
20^2	361	13 (4.9)	711	30 (14.2)	29 (13.6)	28 (13.3)
24^2	529	13 (4.8)	1054	29 (11.7)	27 (10.6)	26 (10.3)
H/h	Test 2: $N = 64$, $H/\delta = 4$, $\rho = 1$					
8	49	14 (4.9)	93	25 (10.3)	25 (10.3)	25 (10.2)
16	49	14 (6.1)	93	27 (11.6)	26 (11.2)	25 (10.9)
32	49	15 (6.4)	93	29 (12.4)	28 (11.6)	26 (10.9)
64	49	15 (6.5)	93	32 (13.9)	30 (12.1)	27 (10.9)
H/h	Test 3: $N = 64$, $H/\delta = 4$, ρ disc					
8	49	23 (9.0)	93	24 (8.6)	24 (8.1)	24 (8.2)
16	49	24 (10.8)	93	27 (9.8)	26 (8.8)	25 (8.3)
32	49	25 (13.0)	93	30 (12.0)	27 (9.7)	26 (8.2)
64	49	27 (15.0)	93	35 (15.9)	29 (11.4)	26 (8.2)

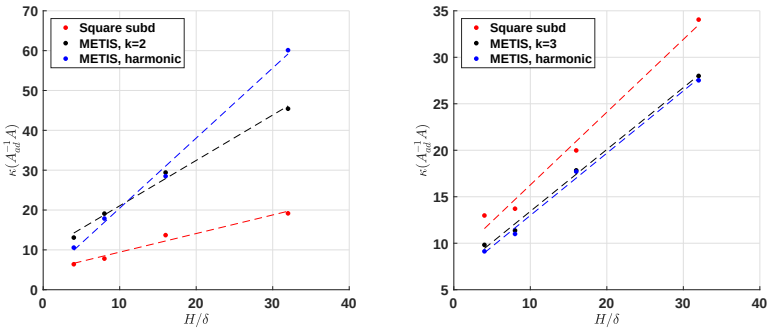

Fig. 5: Condition number as a function of H/δ for a triangular mesh with $N = 64$, $H/h = 32$, $\rho = 1$ (left) and ρ discontinuous (right). The stiffness matrix has 66049 degrees of freedom, N_V is 49 and 95 for square and METIS subdomains, respectively.

H/δ respectively.

6.2.4. Discontinuous coefficients across the interface. We conclude with two experiments where we have discontinuities inside the subdomains, even though our theory does not cover these cases. We consider first a distribution ρ_C as in Figure 8a, where four channels go trough the subdomains. We then consider the extreme case of different values ρ_K for each element; see Figure 8b. Results are presented in Table 6, where we have used a square mesh and METIS subdomains.

Table 2: Number of iterations I and condition number κ (in parenthesis) for our problem with bilinear elements (square mesh) and N subdomains. I_2, I_3 and $I_{\mathcal{H}}$ correspond to $k=2$, $k=3$ and discrete harmonic extensions, respectively. N_V is the dimension of the coarse space.

	Square subd		METIS subdomains			
	N_V	$I_2\,(\kappa)$	N_V	$I_2\,(\kappa)$	$I_3\,(\kappa)$	$I_{\mathcal{H}}\,(\kappa)$
N	Test 1: $H/h=16$, $H/\delta=4$, $\rho=1$					
12^2	121	13 (6.0)	241	22 (7.8)	22 (7.8)	21 (7.8)
16^2	225	12 (6.5)	450	22 (7.9)	22 (7.7)	21 (7.5)
20^2	361	12 (6.7)	721	23 (7.7)	22 (7.5)	21 (7.2)
24^2	529	12 (6.9)	1058	23 (7.7)	22 (7.7)	22 (7.4)
H/h	Test 2: $N=64$, $H/\delta=8$, $\rho=1$					
8	49	14 (10.9)	96	21 (8.4)	21 (8.5)	21 (8.7)
16	49	15 (10.6)	96	23 (9.0)	22 (9.2)	22 (9.1)
32	49	16 (9.7)	96	25 (10.2)	24 (9.7)	23 (9.1)
64	49	17 (8.3)	96	27 (11.7)	26 (10.5)	23 (9.1)
H/h	Test 3: $N=64$, $H/\delta=8$, ρ disc					
8	49	26 (12.6)	96	27 (9.7)	26 (9.5)	27 (9.4)
16	49	27 (15.2)	96	28 (10.2)	27 (9.8)	27 (9.7)
32	49	29 (17.5)	96	31 (12.2)	30 (10.4)	28 (9.9)
64	49	30 (20.4)	96	35 (19.5)	32 (12.2)	29 (10.0)

Table 3: Number of iterations I and condition number κ (in parenthesis) for our problem with VEM (square mesh) and N subdomains. I_2, I_3 and $I_{\mathcal{H}}$ correspond to $k=2$, $k=3$ and discrete harmonic extensions, respectively. N_V is the dimension of the coarse space.

	Square subd		METIS subdomains			
	N_V	$I_2\,(\kappa)$	N_V	$I_2\,(\kappa)$	$I_3\,(\kappa)$	$I_{\mathcal{H}}\,(\kappa)$
N	Test 1: $H/h=16$, $H/\delta=4$, ρ disc					
12^2	121	29 (12.3)	241	27 (9.9)	26 (8.9)	26 (8.7)
16^2	225	30 (12.8)	450	27 (9.5)	26 (8.7)	25 (7.9)
20^2	361	32 (13.5)	721	29 (10.5)	26 (8.5)	25 (7.9)
24^2	529	33 (14.4)	1058	31 (11.1)	29 (10.2)	28 (9.9)
H/h	Test 2: $N=64$, $H/\delta=8$, ρ disc					
8	49	23 (11.4)	96	27 (9.7)	27 (9.5)	27 (9.5)
16	49	24 (14.7)	96	28 (10.2)	27 (9.7)	27 (9.7)
32	49	26 (17.6)	96	31 (12.2)	30 (10.4)	28 (9.9)
64	49	26 (20.4)	96	35 (19.5)	32 (12.2)	29 (10.0)

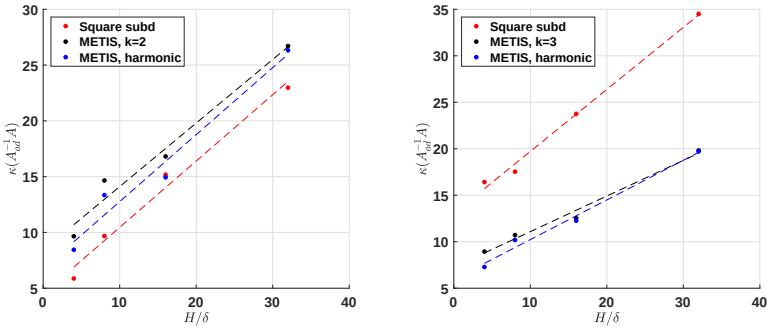

Fig. 6: Condition number as a function of H/δ for a square mesh discretized with VEM. $N = 64$, $H/h = 32$, $\rho = 1$ (left) and ρ discontinuous (right). The stiffness matrix has 66049 degrees of freedom, N_V is 49 and 96 for square and METIS subdomains, respectively.

Table 4: Number of iterations and condition number (in parenthesis) with hexagonal and irregular elements and METIS subdomains. N_V is the dimension of the coarse space, N the number of subdomains, $k = 2$, $H/h \approx 8$ and $H/\delta \approx 4$.

	Hexagonal elements			Irregular elements		
		$\rho = 1$	ρ disc		$\rho = 1$	ρ disc
N	N_V	$I_2\,(\kappa)$	$I_2\,(\kappa)$	N_V	$I_2\,(\kappa)$	$I_2\,(\kappa)$
12^2	239	20 (7.1)	24 (7.8)	203	24 (9.1)	26 (10.3)
16^2	450	20 (6.1)	25 (8.4)	398	23 (8.9)	28 (10.0)
20^2	723	20 (6.2)	24 (7.3)	580	25 (9.9)	32 (13.3)
24^2	1064	21 (7.2)	26 (8.0)	983	36 (10.0)	33 (13.0)

Table 5: Number of iterations and condition number (in parenthesis) with hexagonal and irregular elements and METIS subdomains. N_V is the dimension of the coarse space, $k = 3$, $N = 16$ and $H/\delta \approx 4$.

	Hexagonal elements			Irregular elements		
		$\rho = 1$	ρ disc		$\rho = 1$	ρ disc
H/h	N_V	$I_3\,(\kappa)$	$I_3\,(\kappa)$	N_V	$I_3\,(\kappa)$	$I\,(\kappa)$
8	19	16 (4.5)	17 (4.6)	18	20 (7.1)	22 (6.9)
16	18	17 (5.3)	19 (5.2)	19	23 (8.7)	26 (8.9)
32	18	21 (6.7)	23 (6.6)	18	27 (10.3)	27 (10.2)
64	18	21 (6.2)	22 (7.2)	18	29 (11.0)	30 (11.3)

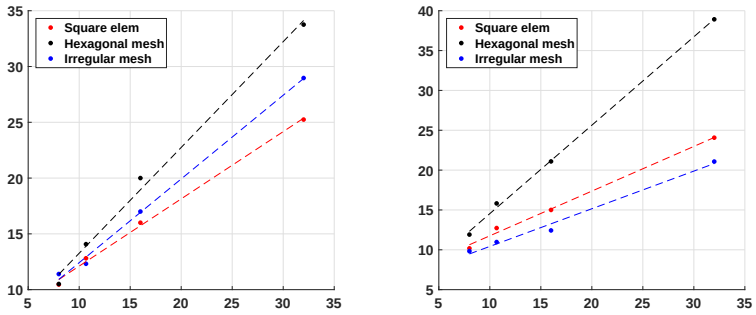

Fig. 7: Condition number as a function of H/δ for different polygonal meshes discretized with VEM. $N = 16$, $H/h = 32$, $\rho = 1$ (left) and ρ discontinuous (right).

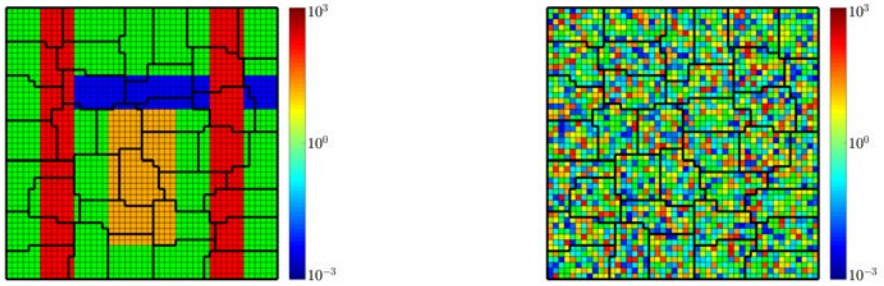

(a) ρ_C (b) ρ_K

Fig. 8: Two discontinuous coefficients ρ considered in Subsection 6.2.4; see results in Table 6a.

Table 6: Number of iterations and condition number (in parenthesis) for our problem with VEM (square elements), METIS subdomains and ρ discontinuous as in Figure 8.

(a) $N = 36$, $H/\delta \approx 3$

H/h	ρ_C $I_3(\kappa)$	ρ_K $I_3(\kappa)$
8	27 (51.9)	43 (87.9)
16	30 (85.3)	47 (101)
32	32 (125)	48 (109)
64	34 (150)	50 (112)

(b) $H/h \approx 16$, $H/\delta \approx 3$

N	ρ_C $I_3(\kappa)$	ρ_K $I_3(\kappa)$
12^2	32 (33.7)	74 (106)
16^2	35 (20.8)	92 (155)
20^2	39 (18.8)	99 (180)
24^2	37 (14.9)	102 (211)

7. Conclusions. In this paper we have introduced a new operator $R_0^T : V_0^R \to V_h$ for approximating virtual coarse functions that belong to the reduced space V_0^R. This approach is particularly useful in the presence of irregular subdomains and relies on the construction of a projector operator into the space of polynomials of a prescribed degree $k \geq 2$. Our approach is faster than previous studies based on discrete harmonic extensions as shown in Figure 3, and provides similar number of iterations and estimates for the condition number of the preconditioned system even for $k = 2$, as confirmed in Section 6.

We have obtained a theoretical upper bound for the condition number of the preconditioned system by using a two-level overlapping Schwarz method, where we have used VEM for the discretization of problem (2). Results are competitive and independent of jumps of the coefficient across the subdomains, and the method allows to handle irregular subdomains as the ones obtained by mesh partitioners. We have also tested cases not covered by our theory in Subsection 6.2.4, where we have discontinuities inside the subdomains. In such cases, a reasonable number of iterations is obtained even for extreme cases of discontinuities and jumps across the elements.

REFERENCES

[1] L. Beirão da Veiga, F. Brezzi, A. Cangiani, G. Manzini, L. D. Marini, and A. Russo, *Basic principles of virtual element methods*, Math. Models Methods Appl. Sci., 23 (2013), pp. 199–214.

[2] L. Beirão da Veiga, F. Brezzi, L. D. Marini, and A. Russo, *The hitchhiker's guide to the virtual element method*, Math. Models Methods Appl. Sci., 24 (2014), pp. 1541–1573.

[3] J. H. Bramble and S. R. Hilbert, *Estimation of linear functionals on Sobolev spaces with application to Fourier transforms and spline interpolation*, SIAM J. Numer. Anal., 7 (1970), pp. 112–124.

[4] S. Brenner and R. Scott, *The Mathematical Theory of Finite Element Methods*, Texts in Applied Mathematics, Springer New York, 2007.

[5] E. Cáceres, *Mixed Virtual Element Methods. Applications in Fluid Mechanics.*, 2015. Thesis (Ph.D.)–Universidad de Concepción, Chile.

[6] J. G. Calvo, *A virtual overlapping Schwarz method for scalar elliptic problems in two dimensions*, Tech. Rep. IM-2017-25, Institute of Mathematics, Czech Academy of Sciences, 2017. Submitted.

[7] C. R. Dohrmann, A. Klawonn, and O. B. Widlund, *Domain decomposition for less regular subdomains: Overlapping Schwarz in two dimensions*, SIAM J. Numer. Anal., 46 (2008), pp. 2153–2168.

[8] C. R. Dohrmann, A. Klawonn, and O. B. Widlund, *A family of energy minimizing coarse spaces for overlapping Schwarz preconditioners*, in Domain decomposition methods in science and engineering XVII, vol. 60 of Lect. Notes Comput. Sci. Eng., Springer, Berlin, 2008, pp. 247–254.

[9] C. R. Dohrmann and O. B. Widlund, *An alternative coarse space for irregular subdomains and an overlapping Schwarz algorithm for scalar elliptic problems in the plane*, SIAM J. Numer. Anal., 50 (2012), pp. 2522–2537.

[10] M. Dryja and O. B. Widlund, *An additive variant of the Schwarz alternating method for the case of many subregions*, Tech. Rep. TR-339, Department of Computer Science, Courant Institute, 1987.

[11] ———, *Some domain decomposition algorithms for elliptic problems*, in Iterative methods for large linear systems (Austin, TX, 1988), Academic Press, Boston, MA, 1990, pp. 273–291.

[12] ———, *Towards a unified theory of domain decomposition algorithms for elliptic problems*, in Third International Symposium on Domain Decomposition Methods for Partial Differential Equations (Houston, TX, 1989), SIAM, Philadelphia, PA, 1990, pp. 3–21.

[13] F. John, *Rotation and strain*, Comm. Pure Appl. Math., 14 (1961), pp. 391–413.

[14] P. W. Jones, *Quasiconformal mappings and extendability of functions in Sobolev spaces*, Acta Math., 147 (1981), pp. 71–88.

[15] G. Karypis and V. Kumar, *A fast and high quality multilevel scheme for partitioning irregular*

graphs, SIAM J. Sci. Comput., 20 (1998), pp. 359–392.
[16] A. Klawonn, O. Rheinbach, and O. B. Widlund, *An analysis of a FETI-DP algorithm on irregular subdomains in the plane*, SIAM J. Numer. Anal., 46 (2008), pp. 2484–2504.
[17] O. J. Sutton, *The virtual element method in 50 lines of MATLAB*, Numerical Algorithms, (2016), pp. 1–19.
[18] A. Toselli and O. B. Widlund, *Domain decomposition methods-algorithms and theory*, vol. 34 of Springer Ser. Comput. Math., Springer, 2005.
[19] O. B. Widlund, *Accommodating irregular subdomains in domain decomposition theory*, in Domain Decomposition Methods in Science and Engineering XVIII, M. Bercovier, M. J. Gander, R. Kornhuber, and O. B. Widlund, eds., vol. 70 of Lecture Notes in Computational Science and Engineering, Springer-Verlag, 2009, pp. 87–98.